

Structural Analysis of $70\text{GeO}_2\text{30Bi}_2\text{O}_3$ Glass by X-ray Diffraction*

Yoshio WASEDA, Kazumasa SUGIYAMA, Yasutada SUNAMORI, Kazuhiko OMOTE¹ and Masahiro ASHIZUKA²
Institute for Advanced Materials Processing, Tohoku University, Sendai 980

¹*Kimura Metamelt Project, ERATO, Research Development Corporation of Japan, Sendai 980*

²*Department of Materials Science and Engineering, Faculty of Engineering, Kyushu Institute of Technology, Kitakyushu 804*

(Received December 28, 1993)

The anomalous X-ray scattering (AXS) technique has been applied to obtain the environmental RDFs around germanium and bismuth in glassy $70\text{GeO}_2\text{30Bi}_2\text{O}_3$ from differential intensities measured at the Ge *K* and Bi *L*_{III} absorption edges using synchrotron radiation. The analysis of the RDFs shows that environmental structure around germanium and bismuth is quite similar to that in $\text{Bi}_4\text{Ge}_3\text{O}_{12}$ crystal. EXAFS analysis is also made in order to confirm the local coordination number of oxygen around the constituent cations. Then, the structural model of glassy $70\text{GeO}_2\text{30Bi}_2\text{O}_3$ was proposed by reproducing the intensity variation measured at Ge *K* and Bi *L*_{III} edges, including the ordinary interference function.

KEYWORDS: X-ray diffraction, anomalous X-ray scattering, EXAFS, germanate glass, $\text{GeO}_2\text{-Bi}_2\text{O}_3$

1. Introduction

Information on physical and chemical properties of glasses is essential for their application to new functional materials. In contrast to crystalline materials, the atomic arrangement in a disordered system like liquids and glasses is not periodic. This leads us to use the so-called radial distribution function (RDF) for structural description. The RDF indicates the probability of finding another atom from an origin as a function of radial distance. This is only one dimensional but almost unique quantitative information demonstrating the atomic arrangements in a disordered system.

The X-ray diffraction is one of the useful techniques for determining the RDF from which the structural parameters such as interatomic distances and coordination numbers can be estimated. However, the ordinary RDF for glasses obtained from a single diffraction profile, is frequently not enough to describe the quantitative structural features in multi-component system because of the poor resolution of some individual peaks of interest. Several new techniques have been developed by applying the near edge absorption phenomena of the constituent elements. The anomalous X-ray scattering method (hereafter to be referred to as AXS) by the so-called anomalous dispersion effect has recently received much attention. The availability of synchrotron radiation has improved the quality of the AXS data and accelerated its application to oxide glass system by obtain-

ing an environmental RDF around a specific atom without any standard materials^{1,2,3}). However, the quality and resolution of each atomic pair in the environmental RDF is, more or less, affected by the scattering power of the co-existing elements and this sometimes causes some inconvenience for obtaining the reliable structural parameters. Germanate or silicate glasses containing heavy metal oxides such as Ti_2O_3 , PbO and Bi_2O_3 are classified into this category and the structural information on cation-oxygen pairs is not easy to obtain. Another technique for analyzing an environmental structure around a specific atom is EXAFS (extended X-ray absorption fine structure), and often used for the local structural analysis of various substances. In spite of many impressive advantages of the EXAFS analysis, structural information for a disordered system cannot be obtained by the simple Fourier transformation of the measured signal alone because of some restrictions arising from the back-scattering amplitude, the phase shift and mean free path of photoelectron⁴). And the lack of the information at low wave-vector part in the EXAFS signal also limits discussion to structure only at small *r* region.

In this context, the $\text{GeO}_2\text{-Bi}_2\text{O}_3$ glassy system is considered as an interesting example of structural study for demonstrating the availability of AXS technique and the construction of a reliable structural model coupled with the EXAFS data. The $\text{GeO}_2\text{-Bi}_2\text{O}_3$ system has extensively been investigated for the application as low-loss fiber-optic and IR transmitting materials⁵). Germanate glasses also show a non-linear change in the molar volume with the addition of

* The 94-R1 report of Institute for Advanced Materials Processing (AMP).

Bi_2O_3 , and this effect has been ascribed to an increase in depolymerization⁶⁾ or the presence of the octahedrally coordinated germanium⁷⁾. Therefore, the environmental structural information around germanium in this glassy system is also strongly required in order to give definite comments on these conflicting prospects.

The main purpose of this article is to present the ordinary and environmental RDFs of $70\text{GeO}_2\text{30Bi}_2\text{O}_3$ glass obtained by the X-ray scattering method. The structural model of glassy $70\text{GeO}_2\text{30Bi}_2\text{O}_3$ is also proposed so as to reproduce the intensity variation measured at Ge K and Bi L_{III} edges, including the EXAFS information.

2. Experimental

Powders of reagent grade bismuth trioxide (Bi_2O_3) and germanium oxide (GeO_2) were mixed in an agate mortar so as to yield nominal compositions of $70\text{GeO}_2\text{30Bi}_2\text{O}_3$. The mixtures were melted in a platinum crucible at about 1250°C in air and corresponding melts were quenched by pouring them on a brass plate. For comparison, GeO_2 , $90\text{GeO}_2\text{10Bi}_2\text{O}_3$ and $80\text{GeO}_2\text{20Bi}_2\text{O}_3$ glasses were also prepared with the similar procedure. Riebling⁶⁾ suggested that GeO_2 more than 60mol% is necessary for glass formation of $\text{GeO}_2\text{-Bi}_2\text{O}_3$. The glass samples presently prepared show orange red in color. The density values were measured by Archimedes' method and are 4.67, 5.89 and 6.56Mg/m^3 for $90\text{GeO}_2\text{10Bi}_2\text{O}_3$, $80\text{GeO}_2\text{20Bi}_2\text{O}_3$ and $70\text{GeO}_2\text{30Bi}_2\text{O}_3$ glasses, respectively.

An ordinary X-ray diffraction profiles was measured using $\text{Mo K}\alpha$ radiation with a pyrolytic graphite monochromator in the diffracted beam up to a value of wave vector $Q(4\pi\sin\theta/\lambda)=135\text{ nm}^{-1}$, where 2θ and λ are the scattering angle and wave length of X-ray, respectively. The measured intensities were corrected for absorption and polarization, and converted into the absolute intensity of $I(Q)$ with the generalized Krough-Moe-Norman method⁸⁾, including the correction for Compton scattering^{9,10)}. The interference functions of $Qi(Q)$ can be obtained from the absolute intensities in the following form;

$$Qi(Q) = \frac{Q(I(Q) - \langle f^2 \rangle)}{\langle f \rangle^2} \quad (1)$$

where $\langle f \rangle$ is the mean atomic scattering factor and $\langle f^2 \rangle$ is the average square of atomic scattering factor¹¹⁾. By Fourier transformation of the function, $Qi(Q)$, the ordinary RDF can be calculated as

$$4\pi r^2 \rho(r) = 4\pi r^2 \rho_0 + \frac{2r}{\pi} \int_0^\infty Qi(Q) \sin Qr dQ \quad (2)$$

The AXS measurement^{1,2,3)} were carried out at a beam line (6B station) in the Photon Factory, National Laboratory for High Energy Physics, Tsukuba, Japan. The incident X-ray is monitored by an N_2 gas ion chamber, so as to maintain the constant incidence irradiating the sample. A pair of X-rays with the energies below Ge K(11.103 keV) and Bi L_{III} (13.424 keV) absorption edges were tuned by using a double Si (111) crystal monochromator for the present AXS measurements. The portable intrinsic pure Ge solid state detector was employed in order to collect both the diffraction and fluorescent intensities from the sample. The measured intensities were corrected using their observed fluorescent intensities^{1,2)}. The energy dependence of measured intensities results mainly from the variation of the real part of the anomalous dispersion term of element A, f'_A ¹²⁾. Therefore, the reduced environmental interference functions for element A, $\Delta i_A(Q)$, may be given by the following equation;

$$\begin{aligned} \Delta i(Q) &= \frac{(I_{E1}(Q) - \langle f_{E1}^2 \rangle) - (I_{E2}(Q) - \langle f_{E2}^2 \rangle)}{c_A(f'_{AE1} - f'_{AE2}) W(Q)} \\ &= \int_0^\infty 4\pi r^2 \sum_{j=1}^3 \frac{\text{Re}[f_{jE1}(Q) + f_{jE2}(Q)]}{W(Q)} \\ &\quad \times (\rho_{Aj} - \rho_{0j}) \frac{\sin(Qr)}{Qr} dr \end{aligned}$$

with

$$W(Q) = \sum_{j=1}^3 c_j \text{Re}(f_{jE1}(Q) + f_{jE2}(Q)) \quad (3)$$

where $I(Q)$ the absolute intensity, c_j and f_j the atomic fraction and X-ray atomic scattering factor of element j , respectively. ρ_{Aj} the number density function of element j around element A, and ρ_{0j} the average number density for the element j . "Re" indicates the real part of the value in the parentheses. The subscripts E1 and E2 represent the incident energies. The summation in the above equation indicates the sum over the constituents of a sample. The environmental RDFs for germanium and bismuth, which represent the local atomic distribution around germanium or bismuth, can be obtained by Fourier transformation of the environmental interference function, $Q\Delta i(Q)$;

$$4\pi r^2 \rho_A(r) = 4\pi r^2 \rho_0 + \frac{2r}{\pi} \int_0^\infty Q \Delta i(Q) \sin Qr dQ \quad (4)$$

The EXAFS measurement were also carried out for Ge K and Bi L_{III} absorption edges on a in-house facility with a combination of a rotating anode-type high power X-ray generator and Johansson-cut Si(100) or (110) monochromator. The usual transmission geometry was applied for the present measurement. The intensity of incident and transmitted X-rays were measured by an Ar ionization chamber and NaI scintillation counter, respectively.

The EXAFS analysis has been widely used for structural studies of various substances and its procedure is now very common¹³. Thus, only essential points employed in this work are given below.

By applying Fourier transformation to the $k^3\chi(k)$ function obtained from the oscillating part in the X-ray absorption ratio beyond its absorption edge, the so-called EXAFS RDF becomes

$$\phi(r) = \frac{1}{\sqrt{2\pi}} \int_0^\infty k^3 \chi(k) \exp(-2ikr) W(k) dk \quad (5)$$

where k the value of wavevector of a photoelectron and $W(k)$ is a window function. This EXAFS RDF provides information about the distribution function of neighboring atoms for a central absorbing atom. On the other hand, the oscillating part of $\chi(k)$ may theoretically be given by the following expression.

$$\chi(k) = \frac{m}{4\pi\hbar^2k} \sum_j \frac{N_j}{r_j^2} t_j(k) \exp\left(\frac{-2r_j}{\lambda_e}\right) \times \sin(2kr_j + \delta_j(k)) \exp(-2k^2\sigma_j^2) \quad (6)$$

\hbar is the Plank constant, m the electron mass. r_j , N_j and σ_j^2 are the interatomic distance, coordination number and its mean square displacement for the element j from an absorbing atom, respectively. $t_j(k)$ is the back-scattering amplitude and $\delta_j(k)$ is the phase shift of the photoelectron, which are calculated by McKale et al.(1988)¹⁴. When mean free path of photoelectrons, λ_e is determined by using standard samples with a known structure, the structural parameters of r , N and σ may be estimated by comparing the calculated spectra using equation (6) with the Fourier filtered experi-

mental spectra obtained by the inverse Fourier transformation of the corresponding pair in the EXAFS RDF.

3. Results and Discussion

The interference functions $Qi(Q)$ of all glass samples obtained by MoK α radiation are shown in Fig. 1. Here, measured intensity data less than $Q=7 \text{ nm}^{-1}$ are smoothly extrapolated to zero at $Q=0 \text{ nm}^{-1}$. The $Qi(Q)$ profile of GeO₂ glass are composed of a set of well resolved peaks at 17 and 27 nm^{-1} followed by a number of peaks at around 45, 63 and 85 nm^{-1} , which implies a corner sharing linkage of GeO₄ tetrahedra^{2,15}. Peaks at 17 and 27 nm^{-1} are converged to a single peak at around 20 nm^{-1} and the others are shifted toward low Q region with increasing Bi₂O₃ content. This suggests the significant structural breakdown of the GeO₄ network mainly arising from the introduction of the larger bismuth atom (0.074 nm) instead of germanium atom (0.053 nm). Slow damping behavior of $Qi(Q)$ function such as GeO₂ glass is popular among oxide glasses and due to a considerable fraction of local ordering unit in their structure. However, this feature becomes inconspicuous with the addition of Bi₂O₃. This may depend upon the decrease in the contribution of local atomic arrangements of GeO₄ to total $Qi(Q)$ functions by introducing the Bi₂O₃ component.

Figure 2 shows the ordinary RDFs and several atomic pairs in crystalline Bi₄Ge₃O₁₂ are indicated by arrows¹⁶. These ordinary RDFs contain six partial structural information of Ge-O, Bi-O, Ge-Bi, Bi-Bi, Ge-Ge and O-O and

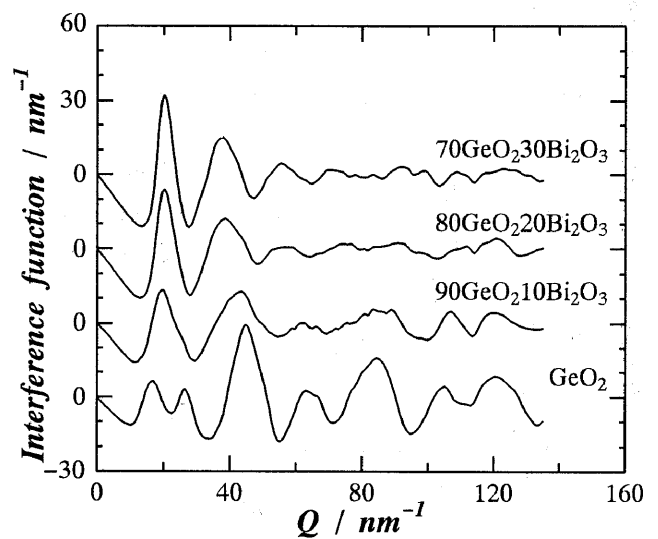


Fig. 1. Interference functions of the glasses in GeO₂-Bi₂O₃ system obtained from the intensity measurements with Mo K α radiation.

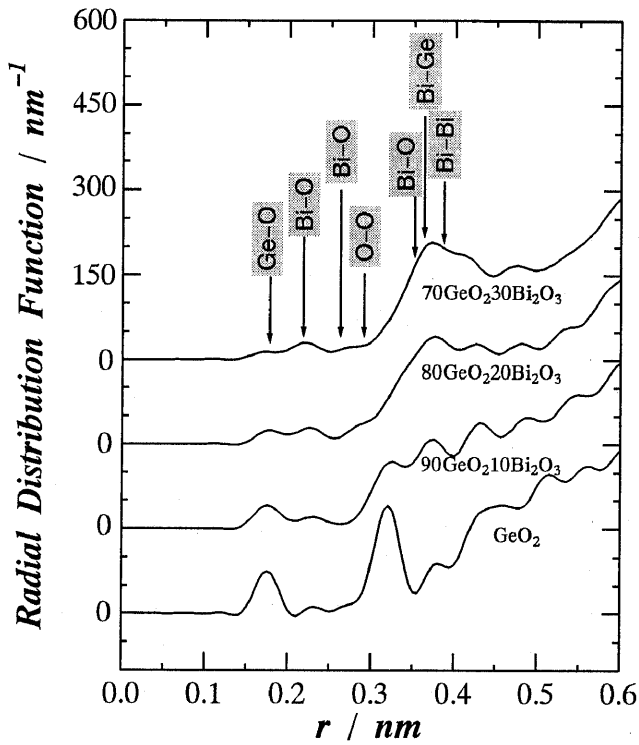


Fig. 2. Ordinary RDF of the glasses in $\text{GeO}_2\text{-Bi}_2\text{O}_3$ system, calculated by Fourier transformation of the interference functions in Fig. 1. The arrows indicate the interatomic distances in the structure of $\text{Bi}_4\text{Ge}_3\text{O}_{12}$ crystal.

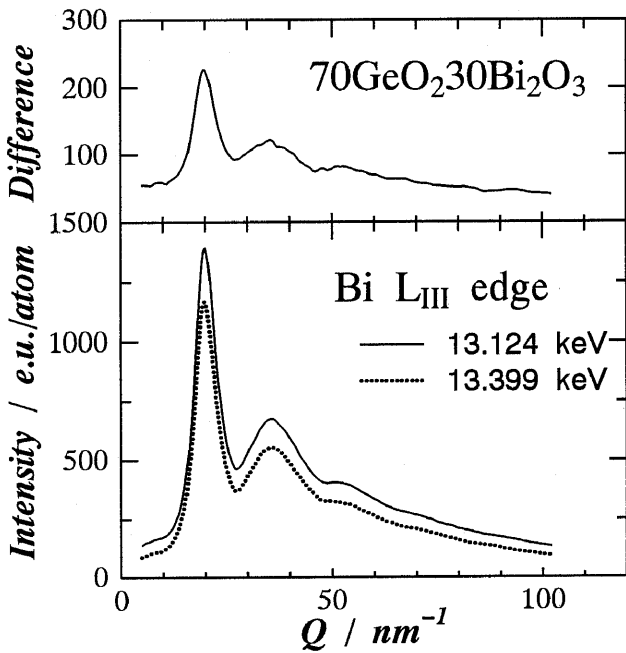


Fig. 3. Differential intensity profile of $70\text{GeO}_2.30\text{Bi}_2\text{O}_3$ glass (top) obtained from the intensity data measured at Bi L_{III} edge (bottom).

detailed structural information is difficult to obtain from these ordinary RDFs alone. Nevertheless, some structural features in these glasses could be drawn as a function of chemical composition. In the case of pure GeO_2 glass, peaks at 0.18 and 0.32 nm are the correlations of the Ge-O and Ge-Ge pairs, respectively^{2,15}. The peak around 0.22 nm is well appreciated by the decrease in the peak height at 0.18 nm with the addition of Bi_2O_3 and this peak is quite likely to correspond to Bi-O pair. However, the so-called termination effect in Fourier transformation, does not allow the exact estimation of the structural parameters of interatomic distance and coordination number for these Ge-O and Bi-O pairs. The intensity of Ge-Ge pair at about 0.32 nm also appears to decrease, while Bi-Ge and Bi-Bi pairs at around 0.35 and 0.40 nm are well recognized with increasing Bi_2O_3 content.

Figure 3 shows two scattering intensity profiles of the $70\text{GeO}_2.30\text{Bi}_2\text{O}_3$ glass measured at two energies near the Bi L_{III} absorption edge, as an example. The differential intensity profile is also given on the top of Fig. 3. The similar differential intensity profile was obtained at Ge K absorption edge. The environmental interference functions around germanium and bismuth for the $70\text{GeO}_2.30\text{Bi}_2\text{O}_3$ glass are shown in Fig. 4, together with the ordinary interference function. Since the environmental function around germanium contains only three partial structural information of

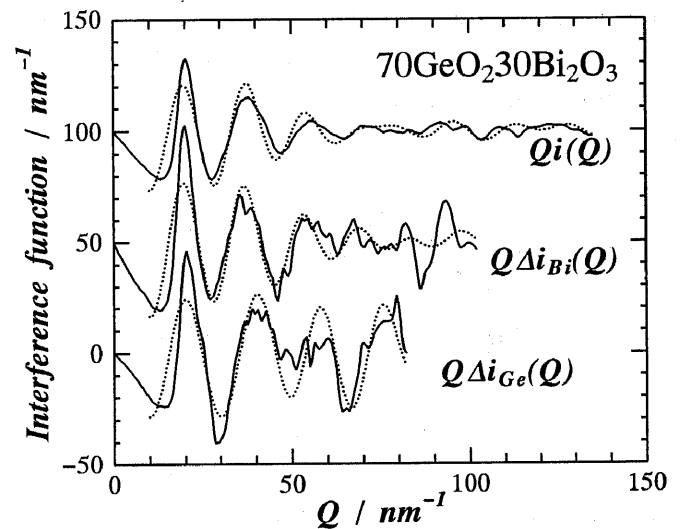


Fig. 4. Environmental interference function of $Q\Delta i_{\text{Ge}}(Q)$ and $Q\Delta i_{\text{Bi}}(Q)$ obtained from the differential intensities measured at Ge K and Bi L_{III} edges, respectively. Ordinary interference function is also shown for comparison. Dotted lines are calculated by using the structural model of $70\text{GeO}_2.30\text{Bi}_2\text{O}_3$ glass (see text).

Ge-O, Ge-Bi and Ge-Ge pairs, and the bismuth case corresponds to the component of Bi-O, Bi-Ge and Bi-Bi, Fourier transformation of each function gives the structural information only around germanium or bismuth atom, respectively. The environmental RDFs calculated by equation (4) are shown in Fig.5 including the ordinary RDF.

The first peak at 0.18 nm in the environmental RDF of germanium is suggested to be the Ge-O correlation and almost resolved. The peak at 0.36 nm appears to be the harmony of the Ge-O, Ge-Ge and Ge-Bi pairs. It may be noticed that the peak at 0.27 nm is considered to be due to the tail of the strong correlation at 0.36 nm. These interatomic distances are consistent with those of crystalline $\text{Bi}_4\text{Ge}_3\text{O}_{12}$, where average Ge-O and Ge-Bi distances are 0.175 and 0.365 nm, respectively¹⁶. Therefore, the local ordering structure around germanium in the $70\text{GeO}_2\text{30Bi}_2\text{O}_3$ glass is suggested to be quite similar to that of crystalline $\text{Bi}_4\text{Ge}_3\text{O}_{12}$. The peak area for the individual atomic pairs in the environmental RDFs corresponds to the coordination number, which could be determined by using the weighting factor of $\text{Re}[f_{J_{E1}}(Q)+f_{J_{E2}}(Q)]/W(Q)$. For example, the weighting factors of $\rho_{\text{Ge-O}}$, $\rho_{\text{Ge-Ge}}$ and $\rho_{\text{Ge-Bi}}$ pairs are calculated as 0.25, 1.11 and 3.67, respectively. This clearly indicates that the contribution of Ge-O pair to the environmental RDF around germanium is considerably small. Thus, it should be remembered that some

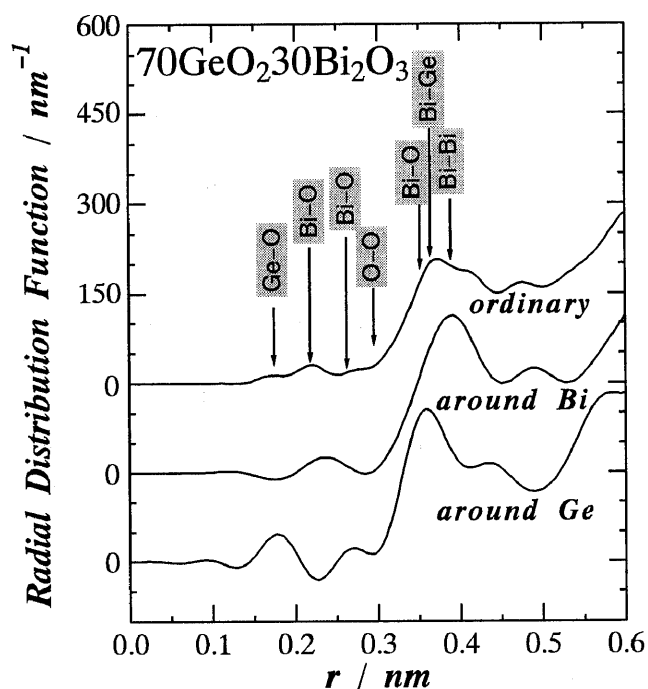


Fig. 5 Environmental RDFs around germanium and bismuth of $70\text{GeO}_2\text{30Bi}_2\text{O}_3$ glass. Ordinary RDF is also shown in comparison.

reservation have to be stressed on the quantitative accuracy of the coordination number of Ge-O pair estimated from present experiment.

As for the environmental RDF around bismuth, the first Bi-O pair at 0.24 nm agrees well with that found in crystalline $\text{Bi}_4\text{Ge}_3\text{O}_{12}$, where bismuth is surrounded by six oxygens with the average distance of 0.24 nm (3 atoms at 0.216 nm and the others at 0.262 nm). The second peak at around 0.39 nm is the harmony of the Bi-O, Bi-Ge and Bi-Bi pairs, which is also comparable to the Bi-Bi distance of 0.389 nm in crystalline $\text{Bi}_4\text{Ge}_3\text{O}_{12}$. This feature again suggests that the local atomic arrangement around bismuth in this glass is similar to that found in the $\text{Bi}_4\text{Ge}_3\text{O}_{12}$ crystal. The weighting factors of $\rho_{\text{Bi-O}}$, $\rho_{\text{Bi-Ge}}$ and $\rho_{\text{Bi-Bi}}$ pairs are 0.27, 1.41 and 3.23, respectively. This allows to determine the coordination numbers for Bi-Ge and Bi-Bi pairs only. It should be worth mentioning that the Bi-O distance of 0.24 nm obtained from the environmental RDF is longer than that of the value of 0.22 nm in ordinary RDF case. This is mainly due to the termination effect of Fourier transformation and this inconsistency can easily be understood when two coordination shells at 0.22 and 0.26 nm for Bi-O pairs in the nearest neighbor region are considered.

The magnitude of the Fourier transformation of the measured spectra $k^3\chi(k)$ at Ge K absorption edge with no phase shift corrections are shown in Fig.6(a), together with those of hexagonal- GeO_2 and $\text{Bi}_4\text{Ge}_3\text{O}_{12}$ crystals. Only a single peak is observed in glassy samples. This peak should be attributed to the first nearest Ge-O pair. Therefore, the structural parameters of a single Ge-O shell could be estimated by comparing the calculated spectra using equation (7) with the experimental one obtained by the inverse Fourier transformation of the first peak area of Ge-O. For the present calculation of $\chi(k)$ functions, the parameter of mean free-path was determined so as to reproduce the correct coordination number of hexagonal- GeO_2 crystal, where germanium is surrounded by four oxygens at a distance of 0.174 nm¹⁷. The resultant values of r , N and σ for Ge-O pairs are listed in Table 1. According to the results of Ge EXAFS, the Ge-O distance of glassy samples in the Bi_2O_3 rich region is slightly longer than those found in hexagonal and glassy GeO_2 . However, the estimated Ge-O distance of 0.178 nm for GeO_4 in crystalline $\text{Bi}_4\text{Ge}_3\text{O}_{12}$ suggests that the change in distance of this system should not be attributed to the change in coordination number around germanium. Thus, the present authors maintain the view that germanium in this glass system appears to form GeO_4 tetrahedron.

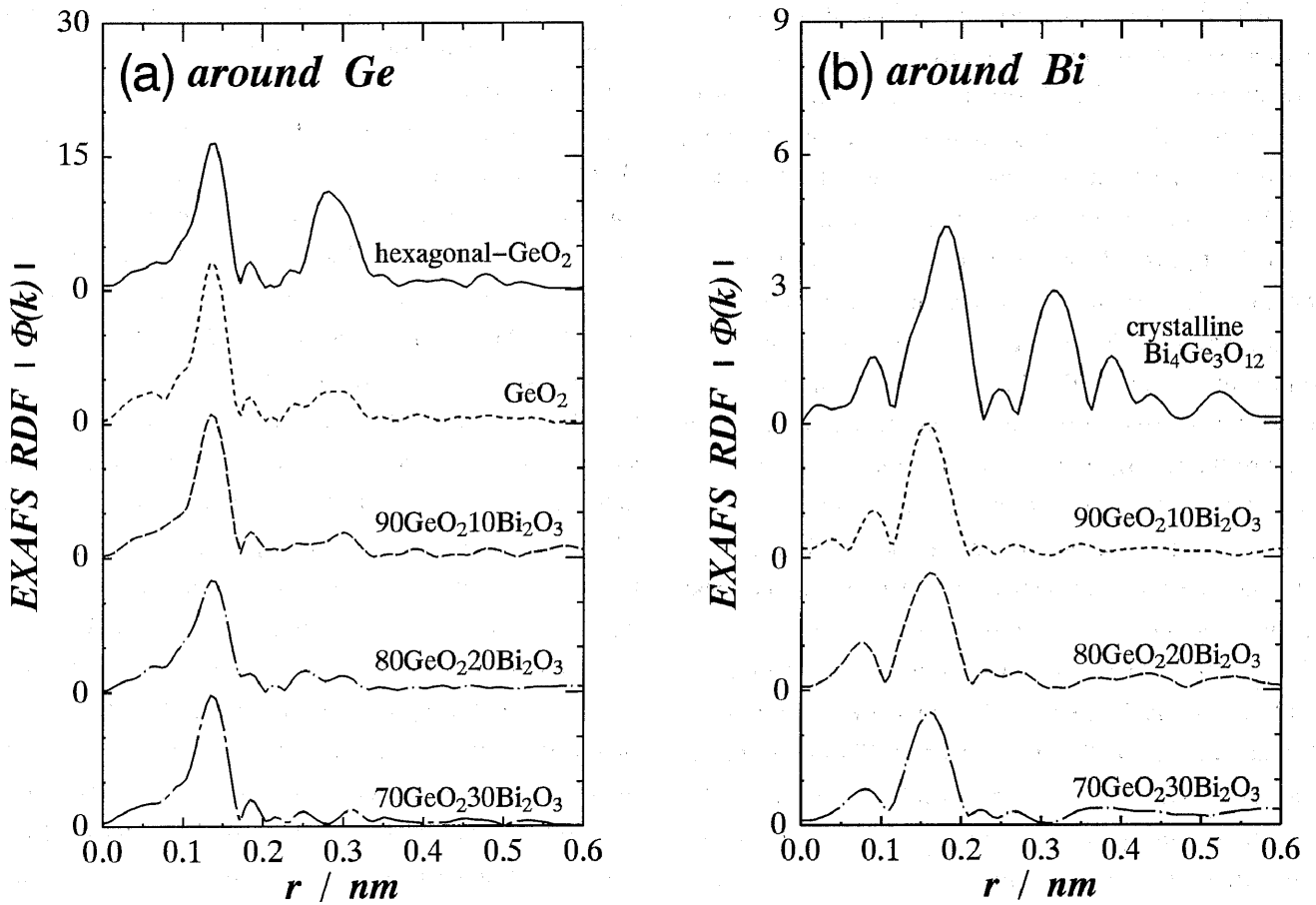


Fig. 6 EXAFS RDF around germanium(a) and bismuth(b) for the glasses in $\text{GeO}_2\text{-Bi}_2\text{O}_3$ system. The results of hexagonal GeO_2 and $\text{Bi}_4\text{Ge}_3\text{O}_{12}$ crystals are also shown.

The EXAFS RDF at Bi L_{III} absorption edge with no phase shift corrections are shown in Fig.6(b), together with that of $\text{Bi}_4\text{Ge}_3\text{O}_{12}$ crystals. The parameter of mean free path for Bi-O pair was fixed so as to obtain the real coordination number in $\text{Bi}_4\text{Ge}_3\text{O}_{12}$ crystal, where three p^3 covalent bonds of 0.216 nm and three coordination by a lone electron pair of 6s at 0.262 nm. Since a single peak appears in the EXAFS RDFs for all glassy samples, it is not so clear that there are two shells of Bi-O coordination as in the $\text{Bi}_4\text{Ge}_3\text{O}_{12}$ crystal. However, X-ray diffraction results rather suggest two coordination shells around bismuth in the glass structure. Therefore, the results of two-shells model are listed in Table 1, although the present authors maintain the view that the reservation may be stressed with the respect to the values of outer shells. The coordination number around bismuth in the present glass system is almost 4 and this is smaller than 6 in $\text{Bi}_4\text{Ge}_3\text{O}_{12}$ crystal. This behavior is quite similar to those of silicate and phosphate glasses including Na_2O , MgO and $\text{CaO}^{18,19}$, and it may be suggested that Bi_2O_3 acts like a network modifier in this system. This is quite feasible when considering that the bonding nature of oxygens in outer shell coordinated by a lone pair of valence electrons of bismuth are likely to be broken first by forming a glass structure. The overall image of the structure in $\text{GeO}_2\text{-Bi}_2\text{O}_3$ glasses can be realized from these information coupled with the EXAFS data. Here, the full structural model of $70\text{GeO}_2\text{30Bi}_2\text{O}_3$ glass is tested by calculating the experimental interference functions.

According to Narten and Levy²⁰, the interference function may be given by the following expression.

$$\begin{aligned}
 Qi(Q) = & \sum_{j=1}^M \sum_k c_j \frac{f_j f_k N_{jk}}{\langle f \rangle^2 r_{jk}} \exp(-b_{jk} Q^2) \sin Qr_{jk} + \sum_{\alpha=1}^M \sum_{\beta=1}^M c_{\alpha} c_{\beta} \frac{f_{\alpha} f_{\beta}}{\langle f \rangle^2} \\
 & \times \exp(-b'_{\alpha\beta} Q^2) 4\pi\rho_0 \frac{Qr_{\alpha\beta} \cos(Qr'_{\alpha\beta}) - \sin(Qr'_{\alpha\beta})}{Q^2}
 \end{aligned} \tag{7}$$

where N_{jk} is the coordination number of atom k around atom j at the distance of r_{jk} and the value of b_{jk} is the mean square variation. The quantities of $r'_{\alpha\beta}$ and $b'_{\alpha\beta}$ correspond to the mean and the variance of the boundary region. The first and second terms of equation (7) represent a discrete Gaussian-like distribution and a continuous distribution with an average number density in longer distance, respectively. The structural parameters in near neighbor correlations are determined by a least-squares analysis with equation (7) so as to reproduce the experimental interference function. The differential interference functions can be readily calculated by taking the difference between the ordinary functions similarly estimated for the AXS measurements at the two energies and compared with the experimental data¹⁵⁾.

The present results suggest that the structural feature of $70\text{GeO}_2\text{30Bi}_2\text{O}_3$ is rather close to that of the $\text{Bi}_4\text{Ge}_3\text{O}_{12}$ crystal. However, it should be kept in mind that the chemical composition of $70\text{GeO}_2\text{30Bi}_2\text{O}_3$ is not identical to the $\text{Bi}_4\text{Ge}_3\text{O}_{12}$ case. Therefore, an initial structural model is constructed as chemically weighted hypothetical structure between the hexagonal GeO_2 ¹⁷⁾ and $\text{Bi}_4\text{Ge}_3\text{O}_{12}$ crystals. After the several iteration of least-squares calculation, the interference functions denoted by dots in Fig.5 were obtained and the resultant structural parameters are listed in Table 2. For convenience, the structural parameters of hexagonal GeO_2 and $\text{Bi}_4\text{Ge}_3\text{O}_{12}$ crystals are also shown in Table 2. In the present calculation, the structural parameters for the first neighboring Ge-O and Bi-O pairs were taken from the EXAFS data and others except for Ge-Ge, Bi-Ge and Bi-Bi pairs at around 0.35 nm were fixed to the values suggested by a starting model. However, such restriction

Table 1. The nearest neighbor correlations estimated from Ge and Bi EXAFS.

	Ge-O		Bi-O(1)		Bi-O(2)	
	$r(\text{nm})$	N	$r(\text{nm})$	N	$r(\text{nm})$	N
hexagonal- GeO_2	0.176	4.0*				
glass GeO_2	0.175	4.0				
$90\text{GeO}_2\text{10Bi}_2\text{O}_3$	0.177	3.9	0.213	2.2	0.258	1.7
$80\text{GeO}_2\text{20Bi}_2\text{O}_3$	0.178	4.2	0.215	2.4	0.258	1.7
$70\text{GeO}_2\text{30Bi}_2\text{O}_3$	0.178	4.3	0.215	2.1	0.266	1.3
$\text{Bi}_4\text{Ge}_3\text{O}_{12}$ crystal	0.178	4.3	0.214	3.0*	0.258	3.0*

* fixed so as to determine parameters of mean free path for photoelectrons.

appears to cause no significant change in structural parameters determined here, because the contribution of Ge-O, Bi-O and O-O pairs are not so large in comparison with cation-cation pairs as discussed before. The most striking result of the present calculation is the missing of linkage of GeO_4 tetrahedra, suggesting GeO_4 tetrahedra are surrounded only by bismuth in the $70\text{GeO}_2\text{30Bi}_2\text{O}_3$ glass. This feature is again quite similar to the structure of $\text{Bi}_4\text{Ge}_3\text{O}_{12}$, where GeO_4 tetrahedra are isolated by the coordination polyhedra around bismuth.

This structural model should be considered to be possible one which explains all the structural experiments demonstrated here, although it might be far from complete. Nevertheless, the present X-ray diffraction analysis coupled with the EXAFS data clarifies the structural features in GeO_2 - Bi_2O_3 glass system. This indicates the overall preference of GeO_4 tetrahedra in this glass system with compositions presently investigated and the depolymerization of GeO_4 linkage by the addition of Bi_2O_3 so as to form a similar structure as the $\text{Bi}_4\text{Ge}_3\text{O}_{12}$ crystal case. Further structural studies by energy-dispersive X-ray diffraction and/or neutron diffraction are also interesting by making available the high resolution RDFs. Such experimental approach is now ongoing.

Table 2. Structural parameters of the local atomic arrangements for glassy $70\text{GeO}_2\text{30Bi}_2\text{O}_3$, together with hexagonal GeO_2 and $\text{Bi}_4\text{Ge}_3\text{O}_{12}$ crystals.

	$70\text{GeO}_2\text{30Bi}_2\text{O}_3$		$h\text{-GeO}_2$		$\text{Bi}_4\text{Ge}_3\text{O}_{12}$	
Density (Mg/m^3)	6.56		3.64		7.11	
i - j pair	$r(\text{nm})$	N	$r(\text{nm})$	N	$r(\text{nm})$	N
Ge-O	0.177	4.0*	0.174	4.0	0.175	4.0
Ge-O	0.350	4.0+	0.348	4.0	0.351	4.0
Ge-O	0.446	12.4+	0.428	14.0	0.446	12.0
Bi-O	0.215	2.2*			0.217	3.0
Bi-O	0.262	1.3*			0.262	3.0
Bi-O	0.363	2.4+			0.363	3.0
Bi-O	0.418	4.8+			0.418	6.0
Ge-Ge	----	0.0	0.315	4.0		
Bi-Ge	0.352	3.7			0.365	6.0
Bi-Bi	0.391	3.3			0.389	3.0
O-O	0.293	7.6+	0.284	6.0	0.296	8.0

* the values obtained by EXAFS RDF.

+ the values estimated by the structures of glass- GeO_2 and $\text{Bi}_4\text{Ge}_3\text{O}_{12}$.

Acknowledgments.

The authors thank the staffs in Photon Factory, National Laboratory for High Energy Physics, Dr.M.Nomura and K.Koyama for their advises of AXS measurements. Technical assistance of E.Ishida of Kyusyu institute of Technology is also greatly appreciated.

Addendum

In recent report of EXAFS measurement²¹⁾, we noted that the preference of GeO₄ tetrahedra is also suggested in the GeO₂-Bi₂O₃ glass system.

- 1) Y.Waseda, E.Matsubara and K.Sugiyama: Sci. Rep. RITU., **34A** (1987) 1.
- 2) E.Matsubara, K.Harada, Y.Waseda and M.Iwase: Z. Naturforsch., **43a** (1988) 181.
- 3) K.Sugiyama, Y.Waseda and M.Ashizuka: Mat. Trans. JIM. **32** (1991) 1030.
- 4) P.A.Lee, P.H.Citrin, P.Eisenberger and B.M.Kincaid: Rev. Mod. Phys., **53** (1981) 61.
- 5) K.Nassau, D.L.Chadwick and A.E.Miller: J. Non-Cryst. Solids **93** (1987) 115.
- 6) E.F.Riebling: J. Mat. Sci. **9** (1974) 753.
- 7) J.A.Topping, N.Cameron and M.K.Murthy: J. Am. Ceram. Soc., **57** (1974) 519.
- 8) C.N.J.Wagner, H.Ocken and M.L.Joshi: Z. Natureforsch., **20a** (1965) 325.
- 9) D.T.Cromer and J.B.Mann: J. Chem. Phys., **47** (1967) 1892.
- 10) D.T.Cromer: J. Chem. Phys., **50** (1969) 4857.
- 11) *International Tables for X-ray Crystallography Vol.IV*, The Knoch Press, Birmingham (1974).
- 12) Y.Waseda: *Novel Application of Anomalous X-ray Scattering for Structural Characterization of Disordered Materials*, Springer-Verlag, New York (1984).
- 13) B.K.Teo: *EXAFS Basic Principles and Data Analysis*, Springer-Verlag, Heiderberg (1986).
- 14) A.G.Mckale, B.W.Veal, A.P.Paulikas, S.K.Chan and G.S.Knapp: J. Am. Chem. Soc., **110** (1988) 3763.
- 15) K.Sugiyama and E.Matsubara: High Temp. Mater. Proc. **10** (1992) 177.
- 16) S.F.Radaev, L.A.Muradyan, Y.F.Kargin, V.A.Sarin, V.N.Kanepit and V.I.Simonov: Sov. Phys. Cryst., **35** (1990) 204.
- 17) S.Gordon, S.Smith and P.B.Isaacs: Acta Cryst., **17** (1964) 847.
- 18) Y.Waseda and H.Suito: ISIJ Inter., **17**(1977) 82.
- 19) Y.Waseda, E.Matsubara, K.Sugiyama, I.K.Suh, T.Kawazoe, O.Kasu, M.Ashizuka and E.Ishida: Sci. Rep. RITU., **35A** (1990) 19.
- 20) A.H.Narten and H.A.Levy: Science, **165** (1969) 447.
- 21) P.P.Lottici, I.Manzini, G.Antonioli, G.Gnappi and A.Montenro: J. Non-Cryst. Solids, **159** (1993) 173.